

Image-Guided Distal Radius Osteotomy Using Patient-Specific Instrument Guides

Manuela Kunz, PhD, Burton Ma, PhD, John F. Rudan, MD, Randy E. Ellis, PhD, David R. Pichora, MD

In this article, we describe a method for computer-assisted distal radius osteotomies in which computer-generated, patient-specific plastic guides are used for intraoperative guidance. Before surgery, the correction and plate location are planned using computed tomography scans for both radii and ulnae, and the planned locations of the distal and proximal drill holes for the plate are saved. A plastic, patient-specific instrument guide is created using a rapid prototyping machine into which a mirror image of intraoperative, accessible bone structure of the distal radius is integrated. This allows for unique positioning of the guide during surgery. For each planned drill location, a guidance hole is incorporated into the guide. During surgery, a conventional incision is made, and the guide is positioned on the radius. The surgeon drills the holes for the plate screws into the intact radius and performs the osteotomy using the conventional technique. Using the predrilled holes, the surgeon affixes the plate to the radius fragments. The guides are easy to integrate into the surgical workflow and minimize the need for intraoperative fluoroscopy for guidance of the procedure. (*J Hand Surg* 2013;38A:1618–1624. Copyright © 2013 by the American Society for Surgery of the Hand. All rights reserved.)

Key words Distal radius osteotomy, image-guided surgery, patient-specific instrument guides.

DISTAL RADIUS FRACTURES are commonly seen injuries in emergency departments.¹ Late complications for this type of fracture include compression neuropathy, posttraumatic arthritis, and malunion.^{2–5} Malunions may cause pain, osteoarthritis, and reduced range of motion or reduced grip strength.^{6–9} Distal radius osteotomy is frequently the preferred surgical treatment to restore normal anatomical relationship in the distal radioulnar and/or radiocarpal joint. In most cases, the radius deformity includes shortening, and therefore a distracting or opening-wedge osteotomy

is needed to correct the alignment. Thorough preoperative planning and understanding of the 3-dimensional abnormalities of the wrist are essential for a successful distal radius osteotomy.

Research has shown that, during surgery, it is essential to replicate the plan accurately and consistently to achieve good postoperative outcomes.^{10,11} This article presents a method in which patient-specific instrument guides are used to navigate the alignment of the distal and proximal fragments with respect to a preoperative plan, as well as to assist with the fixation of the plate to achieve the planned realignment.

TECHNIQUE

Before surgery, a computed tomography (CT) scan is obtained of both forearms, which includes the entire radius and ulna.

Three-dimensional, virtual surface models of the radius and ulna from both affected and unaffected sides are created, using the commercially available software package Mimics (Materialise, Leuven, Belgium). The CT images have an initial automatic segmentation using a lower threshold of 226 and an upper threshold of 3070

From the Department of Surgery, the School of Computing, and the Department of Mechanical and Materials Engineering, Queen's University, Kingston, ON; Department of Computer Science and Engineering, York University, Toronto, ON, Canada.

Received for publication November 20, 2012; accepted in revised form May 19, 2013.

No benefits in any form have been received or will be received related directly or indirectly to the subject of this article.

This work was supported in part by the Canadian Institutes for Health Research, the Canada Foundation for Innovation, and the Natural Sciences and Engineering Research Council of Canada.

Corresponding author: Manuela Kunz, Human Mobility Research Centre, Kingston General Hospital, Agenda 2, Kingston, ON K7L 2V7, Canada; e-mail: kunz@queensu.ca.

0363-5023/13/38A08-0030\$36.00/0
<http://dx.doi.org/10.1016/j.jhssa.2013.05.018>

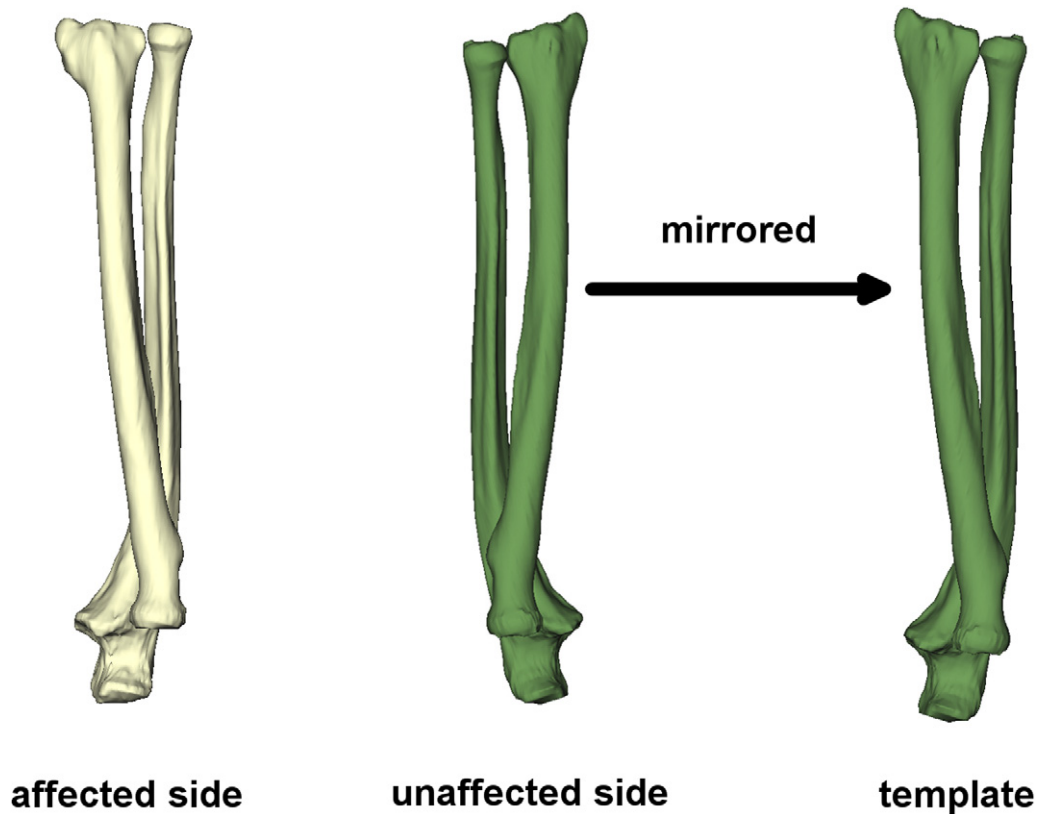


FIGURE 1: Three-dimensional surface models for the affected and unaffected radius and ulna. The unaffected side is mirrored to serve as a template for the correction.

Hounsfield units. This segmentation is manually refined using various editing functions of Mimics. When the segmentation is finished, isosurface models are created and saved. The radius and ulna model of the unaffected site are mirrored to serve as the template for planning the correction (Fig. 1).

Next, the osteotomy is planned. The virtual surface model for the affected radius and ulna, as well as the model for the template radius and ulna, are loaded into the system and displayed to the user. During an initial alignment step, the entire ulna and the proximal radius of the malunited wrist are aligned with the normal template. A virtual cutting plane is chosen within the region of the malunion. Based on the selected cutting plane, a virtual osteotomy of the deformed radius is performed. The distal fragment of the malunited radius is then aligned with the distal part of the template radius (Fig. 2A). When the surgeon is satisfied with the new alignment for the deformed radius, a computer-aided-design file-based model of the fixation plate is virtually placed on the corrected radius model in the desired position for *in vivo* fixation of the bone fragments in place. The surgeon verifies the size, type, and position of the plate, as well as the screw locations to fixate the plate (Fig. 2B). In a final step, the virtual locations of

the screw holes for the plate are saved. Those screw locations are reverse-engineered onto the pre-osteotomy model by applying the inverse transformation of the distal fragment to the locations of the screw holes (Fig. 2C).

The next step involves using custom-made software to calculate a model of the individualized instrument guide. The virtual model of the pre-osteotomy deformed radius and the planned screw positions and orientations are loaded and displayed to the user. A registration surface is selected on the distal radius. The position and size of the registration surface is chosen with respect to the selected surgical approach in such a way that the required surface is safely accessible during the surgery. Furthermore, the registration surfaces are selected in areas that contain a sufficient number of distinctive anatomical landmarks to allow for a unique positioning of the guide during surgery. Figure 3A shows a typical selected registration area for a volar approach.

A mirror image of the selected registration surface is calculated and incorporated into a virtual template model, using a custom-made intersection algorithm (Figs. 3A–3C). For each screw location, a drill guide channel, located and oriented with respect to the preoperative surgical plan, is inserted into the virtual template (Fig. 3D). In a final

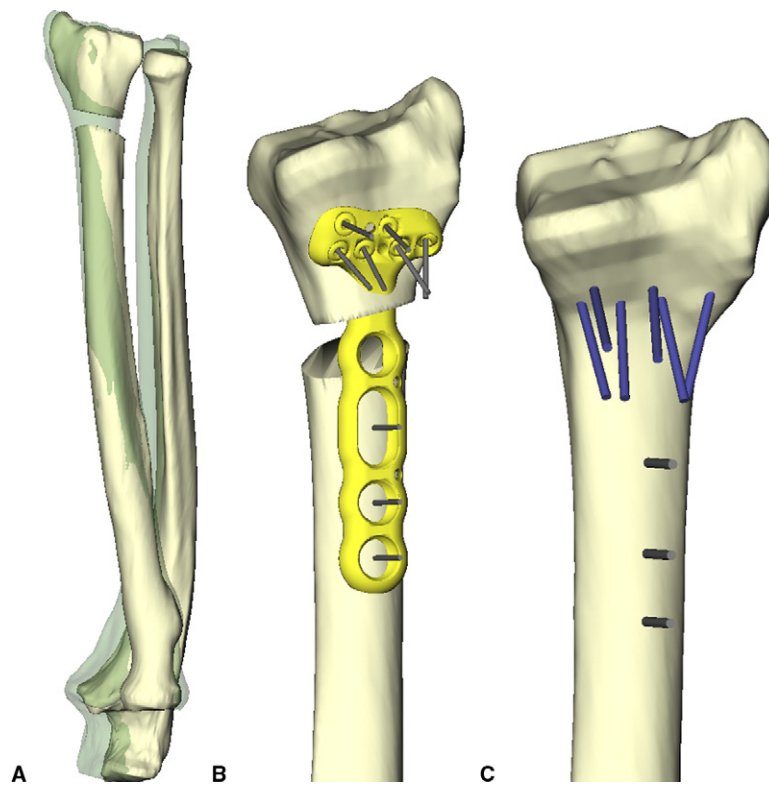


FIGURE 2: Surgical planning. **A** Virtual osteotomy of the radius. The template is superimposed as a transparent model. **B** Placement of the virtual plate and definition of the screw positions and orientations. **C** Saving of screw positions and locations. The distal screw locations are recorded with respect to the intact radius by applying the inverse correction of the distal fragment to the screw locations.

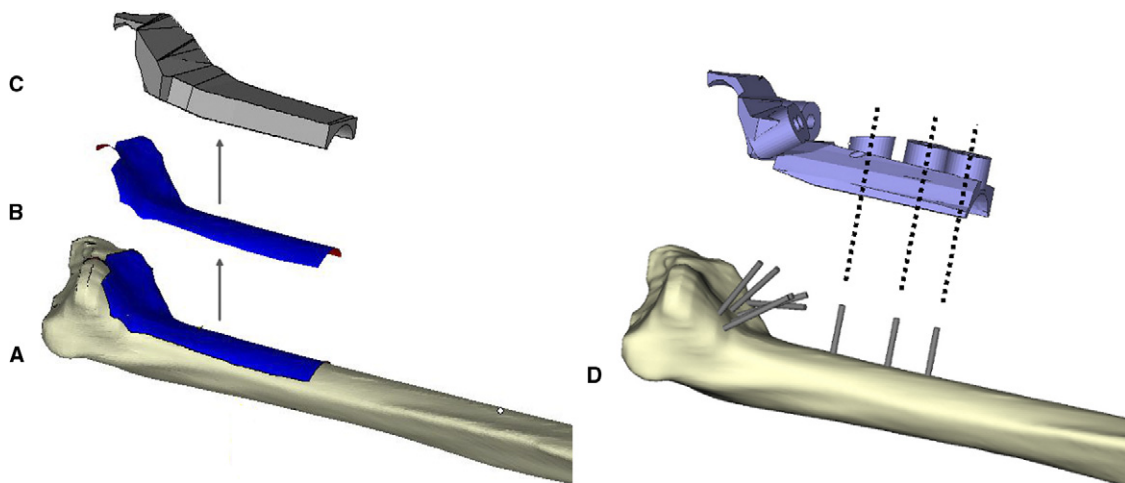


FIGURE 3: Creation of patient-specific instrument guide. **A** Selection of the registration surface. **B** Extracting the mirror image of the registration surface. **C** Integration of the mirror bone image into the patient-specific template. **D** Integration of the instrument guidance into the template with respect to the planned screw location.

step, 2-mm holes for temporary Kirschner wire fixation of the guide to the radius are inserted into the guide in such a way that the Kirschner wire will not interfere with drilling of the screw holes.

When the design of the individualized drilling guide is complete, the computer model data are saved in a

stereolithographic format, and a physical model of the guide is created using a rapid prototyping machine (Dimension SST; Stratasys, Inc., Eden Prairie, MN, USA). The material used during this 3-dimensional printing process is thermoplastic acrylonitrile butadiene styrene. In addition, we create a plastic acrylonitrile

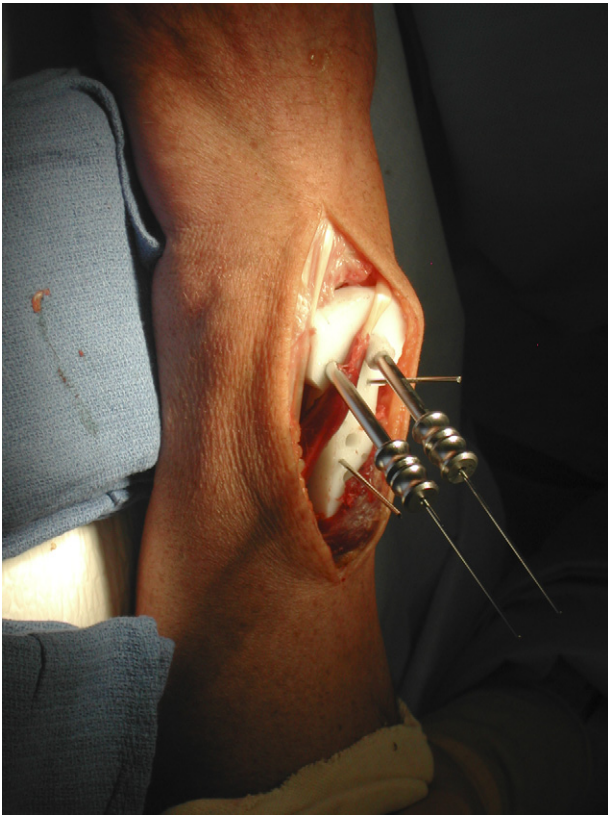


FIGURE 4: Intraoperative procedure. Patient-specific instrument guide is placed on the corresponding bone surface and fixated with two 2-mm Kirschner wires. Metal drill sleeves are inserted into the guidance cylinders, and the screw holes are drilled.

butadiene styrene model of the affected radius. Finally, the individualized drill guide is sterilized by hydrogen peroxide gas plasma, appropriately packed, and labeled before being sent to the operating theater.

The surgeon performs a conventional dorsal or volar approach. After the distal radius is exposed, the surgeon fits the mirror-bone image of the individualized guide to the corresponding bone registration surface, and the guide is secured to the radius using 2-mm (0.079-in) Kirschner wires (Fig. 4; dorsal approach). Metal drill sleeves are inserted into the guidance cylinders of the patient-specific template, and the location is verified with posteroanterior and lateromedial fluoroscopy images. Distal and proximal screw holes are drilled using the patient-specific instrument guide, which is then removed. The osteotomy of the radius is performed with a water-cooled oscillating power saw in the approximate area of the planned virtual osteotomy. The plate is affixed to the distal fragment, using the predrilled screw holes. For an opening-wedge osteotomy, the osteotomy must be generally located between specific plate holes in the vicinity of the malunion, but it does not have to be precisely located. The osteotomy plan is predicated

on the manufacturer's plate design; therefore, the plate must not be contoured during its implantation. Minor trimming of the dorsal fracture callous is usually needed to enable proper plate fitting and to eliminate the need for plate contouring. However, if the osteotomy plane deviates from the planned site, resultant translation of the metaphyseal bone may require more contouring of the metaphyseal cortex and/or callous.

The plate is first fixated to the distal fragment, and then the distal fragment/plate complex is distracted progressively across the osteotomy site with a laminar spreader. When the proximal holes in the plate align with the template-guided drill holes in the proximal radius, the planned alignment is achieved, and the plate fixation can be completed. The remaining screw holes in the plate are fixed with screws in conventional technique. The resulting osteotomy gap is filled with iliac crest cancellous bone graft. This technique is intended for distracting or opening-wedge osteotomies. In the case of shortening or closing-wedge osteotomies, there may be a need for precise location of the osteotomy bone cuts, which may be incorporated into the virtual plan and the template design.

CASE REPORT

A 61-year-old woman sustained a left distal radius fracture during a fall on her outstretched hand. The fracture was treated with closed reduction and casting. She was referred about 8 months later with ongoing difficulties in her left wrist. On examination, the patient had evidence of a distal radius malunion.

Standard posteroanterior and lateral radiographs of the forearm were taken, and the radial inclination (angulation of the distal radial articular surface in the coronal plane), volar tilt (inclination of distal radial articular surface in the sagittal plane), and ulnar variance (length difference between the distal ulna and radius) were measured as described by Mann et al.¹² The radiographic evaluation showed a radial inclination of 22°, a volar tilt of 39°, and 5 mm of positive ulnar variance (Fig. 5). A CT scan of both forearms was performed, and 3-dimensional models of both radii and ulnae were created. The scan was performed with a LightSpeed VCT (GE Healthcare, Waukesha, WI) in helical mode, with a slice thickness of 1.25 mm at 120 kVp. The dose length product was 236.64 mGy-cm. Assuming a conversion factor of $0.28 \times 10^{-2} \text{ mSv(mGy-cm)}^{-1}$ the estimated effective radiation dose was 0.7 mSv.

Using this method, the osteotomy was planned to achieve 26° radial inclination, 4° volar tilt, and -1 mm ulnar variance. Based on the planning for the osteotomy and the 3-dimensional models for the left radius, a



FIGURE 5: Preoperative and postoperative radiographs. Left: preoperative radiographs for the patient. Right: images taken immediately after surgery with the image intensifier.

patient-specific instrument guide was developed, printed, and sterilized.

The intraoperative procedure involved administering general anesthesia to the patient, who was placed in supine position with an arm table and a tourniquet applied to the left arm. A dorsal longitudinal incision overlying the radius tubercle was used. The extensor pollicis longus tendon was identified and mobilized. Dissection down to the dorsal part of the radius was carried out between the third and fourth compartments. The compartments and periosteum were elevated to

expose the underlying radius bone. The exposure was extended distally and proximally to allow adequate visualization of the radius bone. The guide was then fitted to the exposed bone surface, the holes for the screws were drilled, and the guide was removed. The osteotomy and the fixation of the bone fragments were performed as described earlier.

At the end of the surgery, a posteroanterior and lateral image of the wrist using the image intensifier found an alignment of 26° radial inclination, 4° volar tilt, and -2 mm ulnar variance (Fig. 5).

We performed similar procedures (dorsal and volar approach) on 8 additional patients having distal radius osteotomy, with an average follow-up period of 7 months (range, 2 to 22 mo). The average deviation between the achieved and planned radial inclination in these cases was 1.8° (SD, 0.8). For volar tilt, the average deviation between planned and achieved angle was 1.9° (SD, 1.5). The average deviation between the achieved and planned ulnar variance was 0.9 mm (SD, 1.1). All deviations are absolute values between the achieved and planned radiographic parameters and do not represent the direction of the error.

Postoperative complications included one instance of deep infection of the iliac crest, which was successfully treated with irrigations and debridement. In one case, a total wrist arthrodesis was performed 22 months after the distal radius osteotomy due to progressive, posttraumatic arthritis. This complication was related to associated articular surface injury, not the surgical treatment of the extra-articular malunion.

DISCUSSION

Many authors have stressed the importance of accurate planning and execution of the osteotomy.^{11,13–15} The described technique uses patient-specific instrument guides to navigate intraoperative alignment of osteotomy fragments and plate fixation. Our results suggest that patient-specific instrument guides can accurately transfer the preoperative plan into the intraoperative situation. Our preliminary results are comparable to the use of intraoperative opto-electronic tracking of instruments and radius, which is to date considered the gold-standard for image-guided surgery techniques.¹⁶ However, unlike opto-electronic surgical tracking systems, the proposed method requires no additional technical equipment in the operating room, requires no fixation of sensor or markers to the radius or instruments, is easy to integrate into the surgical workflow, and minimizes the need for intraoperative fluoroscopy.

The early cases demonstrate immediate radiographic outcomes that are equivalent to or better than previously published methods and that are within the desired range of outcomes. One may then infer from these results and from the literature that patients are likely to have achieved desirable longer-term clinical outcomes. However, a Level I comparison study needs to be designed and performed to investigate the effect of the use of the proposed technique on the long-term clinical outcome.

Future developments could include the navigation of the osteotomy saw cutting plane and the shaving of the dorsal callous to allow optimal plate fitting. In this

design of opening-wedge osteotomy, the osteotomy does not have to be precisely located. Rather, it must be in the general vicinity of the malunion and optimally located between the proposed fixation plate holes. In most cases, the dorsum of the radius is filled with fracture callous, which matures into solid bone. When the dorsal angulation is corrected in this procedure the callous kicks up, creating a block to the application of a straight (noncontoured) plate. In the procedure described in this article, we perform a free-hand, manual shaving of the dorsal callous to reestablish the original dorsal cortex of the radius. Further improvements might include patient-specific guides to navigate a routing tool for shaving of the distal fragment, as well as supporting the use of custom-contoured plates; these ideas are currently being investigated in laboratory studies.

To date, we have successfully applied this image-guided technique for distal radius osteotomies. However, we believe it may be applicable to other complex deformities of the forearm that can be addressed with an opening-wedge-type osteotomy. Closing-wedge-type osteotomies would likely require further development of the technique for precise navigation of the cutting plane.

We believe that patient-specific instrument guides can provide an accurate and easy-to-use method for image-guided distal radius osteotomies and can improve the intraoperative accuracy of the procedure.

REFERENCES

- Larsen CF, Lauritsen J. Epidemiology of acute wrist trauma. *Int J Epidemiol.* 1993;22(5):911–916.
- Bienek T, Kusz D, Cielinski L. Peripheral nerve compression neuropathy after fractures of the distal radius. *J Hand Surg Br.* 2006; 31(3):256–260.
- Knirk JL, Jupiter JB. Intra-articular fractures of the distal end of the radius in young adults. *J Bone Joint Surg Am.* 1986;68(5):647–659.
- Cooney WP III, Dobyns JH, Linscheid RL. Complications of Colles' fractures. *J Bone Joint Surg Am.* 1980;62(4):613–619.
- McGrory BJ, Amadio PC. Malunion of the distal radius. In: Cooney WP, Linscheid RL, Dobyns JH, eds. *The Wrist: Diagnosis and Operative Treatment.* Vol 1. 1st ed. St. Louis, MO: Mosby; 1998:356–384.
- Jupiter JB, Masem M. Reconstruction of post-traumatic deformity of the distal radius and ulna. *Hand Clin.* 1988;4(3):377–390.
- Overgaard S, Solgaard S. Osteoarthritis after Colles' fracture. *Orthopedics.* 1989;12(3):413–416.
- Taleisnik J, Watson HK. Midcarpal instability caused by malunited fractures of the distal radius. *J Hand Surg Am.* 1984;9(3):350–357.
- Jenkins NH, Mintowt-Czyz WJ. Mal-union and dysfunction in Colles' fractures. *J Hand Surg Br.* 1988;13(3):291–293.
- von Campe A, Nagy L, Arbab D, et al. Corrective osteotomies in malunions of the distal radius: do we get what we planned? *Clin Orthop Relat Res.* 2006;450:179–185.
- Prommersberger KJ, Van Schoonhoven J, Lanz UB. Outcome after corrective osteotomy for malunion fractures of the distal end of the radius. *J Hand Surg Br.* 2002;27(1):55–60.
- Mann FA, Wilson AJ, Gilula LA. Radiographic evaluation of the wrist: What does the hand surgeon want to know? *Radiology.* 1992; 184(1):15–24.

13. Fernandez DL. Correction of post-traumatic wrist deformity in adults by osteotomy, bone-grafting, and internal fixation. *J Bone Joint Surg Am.* 1982;64(8):1164–1178.
14. McQueen M, Caspers J. Colles' fracture: does the anatomical result affect the final function? *J Bone Joint Surg Br.* 1988;70(4):649–651.
15. Aro HT, Koivunen T. Minor axial shortening of the radius affects outcome of Colles' fracture treatment. *J Hand Surg Am.* 1991;16(3):392–398.
16. Athwal GS, Ellis RE, Small CF, et al. Computer-assisted distal radius osteotomy. *J Hand Surg.* 2003;28(6):951–958.